ICARUS **129,** 367–383 (1997)
ARTICLE NO. IS975778

Coupled Orbital and Thermal Evolution of Ganymede

Adam P. Showman

Division of Geological and Planetary Sciences 150-21, California Institute of Technology, Pasadena, California 91125, and Lunar and Planetary Institute, 3600 Bay Area Boulevard, Houston, Texas 77058
E-mail: showman@earth1.gps.caltech.edu

David J. Stevenson

Division of Geological and Planetary Sciences 150-21, California Institute of Technology, Pasadena, California 91125

and

Renu Malhotra

Lunar and Planetary Institute, 3600 Bay Area Boulevard, Houston, Texas 77058

Received April 25, 1996; revised May 5, 1997

We explore the hypothesis that passage through an eccentricity-pumping resonance could lead to the resurfacing of Ganymede. To do so, we couple R. Malhotra's (1991, *Icarus* 94, 399–412) orbital model for the tidal evolution of the Laplace resonance to an internal model of Ganymede. Our model explores the conditions under which Ganymede can undergo global thermal runaway, assuming that the Q/k of Ganymede is strongly dependent on internal temperature. (Here Q is the tidal dissipation function and k is the second-degree Love number.) We allow the system to pass through the $\omega_1/\omega_2 \approx 2$ or $\omega_1/\omega_2 \approx 1/2$ resonance, where $\omega_1 \equiv 2n_2 - n_1$, $\omega_2 \equiv 2n_3 - n_2$, and n_1, n_2, and n_3 are the mean motions of Io, Europa, and Ganymede. If Ganymede's initial internal temperature is either "too hot" or "too cold," no runaway occurs, while for intermediate temperatures (~200 K in the upper mantle), conditions are "just right," and runaway occurs. The range of mantle temperatures that allows runaway depends on the model for tidal Q; we use the Maxwell model, which ties Q to the creep viscosity of ice. Runaways can induce up to ~50–100 K warming and formation of a large internal ocean; they occur over a 10^7 to 10^8-year period. Assuming carbonaceous chondritic abundances of radionuclides in Ganymede's rocky portion, however, we find that the interior cannot cool to the initial temperatures needed to allow large runaways. If our model is correct, large runaways cannot occur, although small runaways are still possible. Different formulations of tidal Q or convective cooling may allow large runaways. Large runaways are also possible if radionuclides are substantially depleted, although this is unlikely.

We next consider the consequences of a large runaway, assuming it can occur. Ganymede can undergo 0.5% thermal expansion (by volume) during the largest thermal runaways. Melting of the ice mantle provides up to 2% expansion despite the fact that contraction produced by melting ice I offsets expansion produced by melting high-pressure ice phases. Solid–solid phase transitions cause negligible satellite expansion. Lithospheric stresses caused by expansion of 2% over 10^7 to 10^8 years are ~10^2 bars at the surface, and drop to a few bars at several kilometers depth. Such stresses could cause cracking to depths of several kilometers. The cracking and near-surface production of warm or partially molten ice make resurfacing a plausible outcome of a large thermal runaway. The tidal heating events proposed here may also be relevant for generation of Ganymede's modern-day magnetic field.

1. INTRODUCTION

Ganymede and Callisto have similar bulk properties but divergent surfaces. Callisto's surface is old and shows little sign of endogenic volcanic or tectonic activity. Half of Ganymede's surface resembles that of Callisto, but the other half was resurfaced long after late heavy bombardment. The differences between the satellites are puzzling, because one might expect that satellites with similar bulk properties would follow similar evolutionary pathways. Understanding why the two satellites evolved so differently is potentially important for understanding icy satellite formation and evolution generally.

There have been many previous attempts to explain why Ganymede but not Callisto might undergo upper mantle activity (e.g., melting), most of which assume the divergent evolutionary paths were caused by small quantitative differences in initial conditions, size, or composition of the two satellites (Squyres 1980, Cassen *et al.* 1980, Schubert

0019-1035/97 $25.00

et al. 1981, McKinnon 1981, Lunine and Stevenson 1982, Friedson and Stevenson 1983, Kirk and Stevenson 1987). Generally, such studies show that one must carefully tune poorly known parameters to get extensive activity in Ganymede but not Callisto. Such mechanisms are therefore unlikely. In addition, these models generally provide no plausible means for transporting material to the surface, even if mantle activity seems likely. A comprehensive review of the problem and early work is given by McKinnon and Parmentier (1986).

Although Ganymede's current eccentricity is low (0.0015), the eccentricity might have been high enough in the past for tidal dissipation to drive internal activity (Showman and Malhotra 1997, Malhotra 1991, Tittemore 1990, Greenberg 1987). The most plausible scenario is that of Malhotra (1991) and Showman and Malhotra (1997), in which Io, Europa, and Ganymede pass through a Laplace-like resonance before evolving into the presently observed Laplace resonance. These authors explored several scenarios by which the Laplace resonance, $\omega_1 = \omega_2$, was established; here $\omega_1 \equiv 2n_2 - n_1$, $\omega_2 \equiv 2n_3 - n_2$, and n_1, n_2, and n_3 are the mean motions (i.e., the mean orbital angular velocities) of Io, Europa, and Ganymede, respectively. They showed that three scenarios, involving temporary capture into a resonance characterized by $\omega_1/\omega_2 \approx 1/2$, 3/2, or 2, pump Ganymede's eccentricity to ~0.01–0.04.

Although the most optimum scenarios of Showman and Malhotra (1997) and Malhotra (1991) produce a mean heating great enough to significantly enhance upper mantle activity, this is untrue in general. Hence, it is unclear how the resonance causes resurfacing. The most violent mean heating rate possible during resonance passage is roughly 10^{13} W (Showman and Malhotra 1997), several times the primordial radiogenic heating rate of 3×10^{12} W occurring in Ganymede's rocky portion (assumed carbonaceous chondritic). This tidal heating rate requires that Q_J be near its time-averaged lower limit of 3×10^4 and that the system pass through the $\omega_1/\omega_2 \approx 2$ resonance, the most powerful of the three eccentricity-pumping Laplace-like resonances. (Here, Q_J is the tidal Q of Jupiter.) However, Q_J is unknown and could greatly exceed 3×10^4, implying a lower heating rate. Further, for a given Q_J, weaker heating would occur if the system passed through $\omega_1/\omega_2 \approx 3/2$ or 1/2 rather than $\omega_1/\omega_2 \approx 2$. For example, passage through the $\omega_1/\omega_2 \approx 1/2$ resonance generates 2×10^{11} W of dissipative heating if $Q_J = 3 \times 10^5$ (Showman and Malhotra 1997, Malhotra 1991). Relative to radiogenic heating, such tidal heating is weak and is unlikely to account for upper mantle activity or resurfacing.

If Q/k changes with time, however, the power dissipated during narrow time intervals can overwhelm radiogenic heating even when mean heating is below radiogenic. The tidal energy dissipation rate within a synchronously rotating satellite in an eccentric orbit is (Peale and Cassen 1978)

$$\dot{E} = \frac{21}{2}\frac{k}{Q}\frac{R^5 G M_p^2 n e^2}{a^6} \approx 2 \times 10^{18}\left(\frac{k}{Q}e^2\right) \text{W}, \qquad (1)$$

where R is the satellite's radius, a, e, and n are the orbital semimajor axis, eccentricity, and mean motion, M_p is the primary's (Jupiter) mass, G is the gravitational constant, Q is the satellite's effective tidal dissipation function, and k is the satellite's second-degree Love number, which parameterizes the height of the tidal bulge relative to the equipotential (Munk and MacDonald 1960); the numerical estimate given in Eq. (1) is for Ganymede. Suppose Q/k begins high (say 10^3), so that e reaches 0.02–0.04 within one of the Laplace-like resonances described by Showman and Malhotra (1997) or Malhotra (1991). If Q/k drops suddenly to 10, the tidal dissipation would be a few $\times 10^{13}$ W, 10 times greater than primordial radiogenic heating. Clearly such an event could make resurfacing far more likely.

Further, the energy released on a large decrease in Q/k is great enough to allow internal activity. The change in Ganymede's orbital energy at constant orbital angular momentum is (for small e) $\Delta E \approx GM_J M e\, \Delta e/a$, where M_J and M are Jupiter's and Ganymede's masses, and Δe is the change in eccentricity. For circularizing the orbit, we take $e \sim \Delta e \sim 0.03$, which gives $\Delta E \approx 2 \times 10^{28}$ J. Complete melting of Ganymede's icy fraction (roughly one-half Ganymede's mass) requires $0.5ML \approx 2 \times 10^{28}$ J, where $L \approx 3 \times 10^5$ J kg^{-1} is the latent heat of melting and M is Ganymede's mass. Thus, if Q/k plummets quickly enough for minimal convective loss of the dissipated energy, massive melting is possible.

We postulate that Ganymede's Q/k depends sensitively on Ganymede's internal temperature and structure, and that Q/k is lower for warm, molten states than for cold, frozen states. This provides a mechanism whereby Q/k can change very rapidly. Suppose Ganymede initially begins cold, with high Q/k. The eccentricity would therefore rise to a high value, thereby increasing dissipation. The warming caused by this dissipation would decrease Q/k slightly, which would increase the dissipation and accelerate the rate of warming and of decrease in Q/k. (This requires Q/k to decrease faster than e^2, so that e^2k/Q increases over time.) Thus, a positive feedback could occur, in which Ganymede undergoes massive ''runaway'' heating and in which e plummets over an extremely short time interval.

In Fig. 1, we illustrate the qualitative effects of such a runaway on Ganymede's structure. Figure 1a schematically displays Ganymede's eccentricity over time during the runaway. Figures 1b to 1e show cross sections of Ganymede's interior at various times during the runaway, marked in Fig. 1a. Suppose the initial state is frozen and differentiated, containing a rock/iron core overlain by a water ice mantle of ice I, III, V, and VI. Because the ice mantle adiabatic

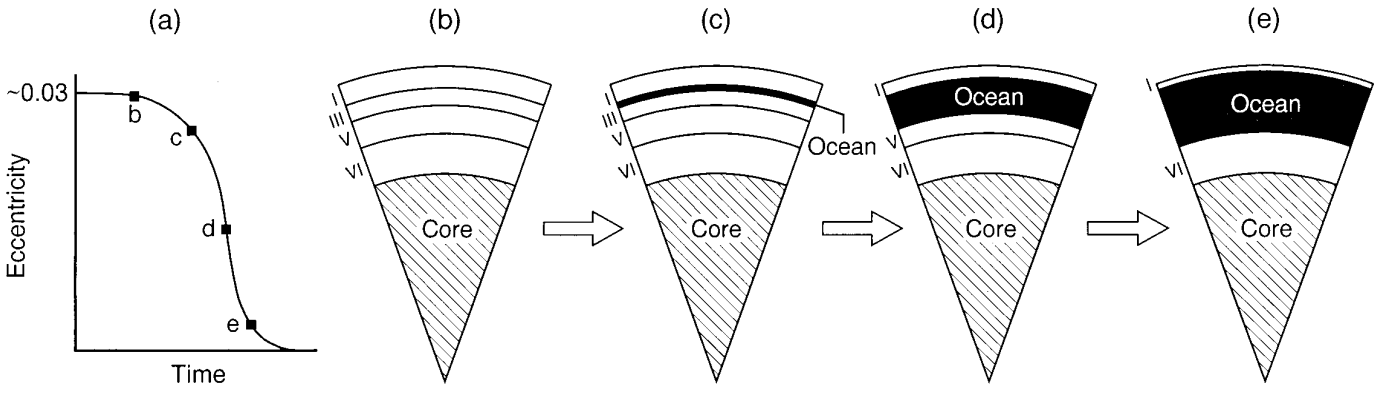

FIG. 1. Qualitative effects of a thermal runaway on Ganymede's structure. (a) Schematic of Ganymede's eccentricity over time during the runaway. (b)–(e) Cross sections of Ganymede at various times during the runaway, as marked in (a). The initially frozen, differentiated Ganymede undergoes melting at the ice I–III interface, leading to formation of a massive internal ocean.

temperature rises only gently with depth, and because the water ice melting temperature minimizes at the ice I–III interface (at 160 km depth), melting begins there, leading to formation of an ocean between these layers. As melting continues, the ocean grows, and both the ice I and III layers decrease in size. Eventually, ice I and V and then ice I and VI melt simultaneously. Alternatively, Ganymede might enter the runaway cold, containing only ices I, II, and VI. The runaway could convert the ice II into ices I, III, and V, leading to a final state similar to that shown in Fig. 1b (see phase diagram in Hobbs 1974). Either of these processes might lead to expansion and possibly lithospheric cracking.

In this paper, we explore the coupled orbital and thermal dynamics of Ganymede to answer several questions: (1) Can thermal runaways occur, and if so, what conditions are necessary for their occurrence? What range of mantle temperatures is needed at the onset of orbital resonance to trigger a runaway? Are such initial mantle temperatures plausible, given likely radiogenic heating and convective cooling rates? (2) How much warming or melting occurs during the runaways? Over what time scale do the runaways occur? (3) What are the implications of the runaways for lithospheric stresses and cracking?

To attack the first two questions, we construct a model of Ganymede's interior, from which we can calculate Q/k. We couple this model to Malhotra's (1991) orbital model, and follow the evolution of Ganymede's orbital and structural characteristics over time in a computer simulation. To answer the third question, we calculate the extent to which Ganymede would expand during a runaway from internal phase changes and thermal expansion. Using this value of strain and the runaway time scales, we can estimate the lithospheric strain rate encountered during the runaway, and solve for the lithospheric stress using the Maxwell equation.

The paper is organized as follows. Section 2 contains a description of the Ganymede thermal model. Section 3 describes the results of the coupled orbital–thermal model. In Section 4 we calculate the satellite expansion caused by runaway, and in Section 5 we calculate lithospheric stress as a function of depth and estimate the depth to which cracking can occur. In Section 6 we discuss the implications of our results for resurfacing. Although we have not modeled the detailed evolution of Ganymede's rock/iron core, the evolution of the ice mantle has important implications for the behavior of the core and, hence, for Ganymede's magnetic field (Kivelson *et al.* 1996). We discuss these at the end of Section 6.

2. MODEL ASSUMPTIONS

We use the model of Malhotra (1991) for the orbital dynamics and tidal evolution of Io, Europa, and Ganymede near the Laplace resonance. The model uses a perturbative expansion of the satellite gravitational interactions with secular and resonant terms up to second order in the satellite eccentricities; the perturbations due to the first two gravitational harmonics of Jupiter are also included. Tidal dissipation in the satellites and Jupiter is parameterized by the ratio Q/k of the tidal dissipation function to second-degree Love number of each body. These ratios were free parameters in Malhotra's (1991) study. The equations of motion are obtained in a set of canonical variables which facilitates the construction of an algebraic mapping. This significantly speeds up numerical simulation of the system's long-term evolution compared with conventional ODE integration schemes.

Even with the mapping method, numerical simulations with realistic values $Q_J \sim 10^5$ require prohibitively long computation times. We thus run the orbital model using $Q_J = 100$, which speeds up the evolution by a factor

$Q_{J_{real}}/Q_{J_{computation}} \sim 10^3$. It is expected (but not rigorously proven) that when the ratios of satellite Q/k to Q_J are specified, the orbital dynamics is exactly the same, but proceeds $\sim 10^3$ times faster. We assume that the large, rapid changes in Q/k Ganymede undergoes (which we have speeded up by a factor of $\sim 10^3$ in the orbital model) do not affect the expected adiabaticity of the orbital evolution; see Malhotra (1991) for discussion.

Nowhere in the orbital model is $Q_{J_{real}}$ specified. However, our thermal model specifies the actual value of Ganymede's Q/k, not a ratio to Q_J. Furthermore, convective cooling rates depend on actual time. In the coupled orbital–thermal model, therefore, we must specify $Q_{J_{real}}$, to fix the actual time axis. We use $Q_{J_{real}} = 3 \times 10^5$.

Our Ganymede interior model calculates both geophysical parameters (such as the size of the ocean) and Q/k over time; we feed the latter into the orbital part of the model. Thus, Ganymede's Q/k is no longer a free parameter (as in Malhotra 1991), but is determined by our thermal model. The Q/k of Io, Europa, and Jupiter are still free parameters.

The concept of the Ganymede model is as follows. By specifying satellite composition and temperature with depth at a given time, we can determine the physical structure (sizes of ice layers and internal oceans). By assuming a model for $Q(T)$ in ice and using the satellite physical and thermal structure, we can calculate the effective Q/k. Given the eccentricity from the orbital model, this specifies the dissipated power through Eq. (1). Coupled with a method for calculating heat loss to space, we can estimate the net heat source or sink within Ganymede, and can then determine how the temperature profile (and therefore physical structure) changes over time. Because the model for Q is so unconstrained, we keep the rest of the thermal model simple.

Here we describe the Ganymede physical model:

i. Bulk Properties

We assume a differentiated Ganymede, consisting of a pure water mantle overlying a rock/iron core. The mass, radius, and gravity (taken to be constant with depth) are 1.5×10^{23} kg, 2640 km, and 1.5 m sec^{-1}. We assume that the ice mantle constitutes half of Ganymede's mass.

The assumption that Ganymede entered the resonance in a differentiated state is consistent with available constraints. The Galileo gravity data imply that Ganymede is strongly differentiated at present (Anderson *et al.* 1996). Thermal models including accretional and radiogenic heating suggest differentiation early in Ganymede's history (Schubert *et al.* 1981, McKinnon and Parmentier 1986). Further, Ganymede's outer layers must have differentiated *before* dark terrain formation. If not, then the crust underlying dark terrain would be primordial and of density

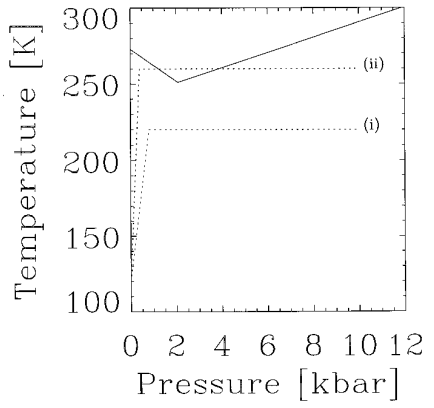

FIG. 2. The water ice melting curve used in the Ganymede thermal model (solid line). Overlain on the melting curve we show two sample model temperature profiles (dotted lines). Each contains a conductive lithosphere and thermal boundary layer, underlain by an isothermal convective region. Case (i) corresponds to a solid Ganymede and case (ii) represents a Ganymede with an internal liquid ocean bounded above and below by ice layers.

~ 1.6 g cm^{-3}. These dense regions, overlying the clean, differentiated ice mantle, would be unstable and would founder over geologic time. The idea that the crust cannot support such large density contrasts is bolstered by the low topography on Ganymede. Therefore, the dark terrain must have a density comparable to that of clean ice, implying differentiation of the outer layers. (The fact that Ganymede's dark terrain has half the crater density of Callisto, despite a higher impactor flux at Ganymede, suggests ancient resurfacing of Ganymede's dark terrain and is consistent with an early differentiation event.) Once differentiation initiates, the heat it produces generally drives it to completion (Friedson and Stevenson 1983). We therefore infer that Ganymede was massively differentiated at or before dark terrain formation 3.5–4 byr ago.

ii. Water Physical Data

We assume a simplified ice melting curve as shown in Fig. 2 (solid line). Each branch of the curve is linear with pressure, and the curve contains one kink, representing the ice I–III–liquid triple point at 2.08 kbar and 251 K. The region to the left of the kink represents the ice I field, and that to the right represents the field of high-pressure polymorphs, ice III, V, and VI.

We use the data on the physical properties of water given in Table I. Because we do not explicitly distinguish between ices II, III, V, and VI, the table shows data for the phases ice I, liquid water, and "high-pressure ice." All the parameters are taken to be constant with pressure.

iii. Satellite Thermal and Physical Structure

We assume Ganymede's ice mantle undergoes solid-state convection, and that there is a rigid, thermally conduc-

TABLE I
Water Physical Data Used in Model

	Liquid	Ice I	"High-pressure ice"
c_p (J kg^{-1} K^{-1})	4218	2000	2000
L (J kg^{-1})	—	3×10^5	3×10^5
ρ (kg m^{-3})	1000	1000	1000
α (K^{-1})	—	1.5×10^{-4}	—
κ (m^2 sec^{-1})	—	10^{-6}	—
dT_m/dp (K Pa^{-1})	—	-1.0577×10^{-7}	5×10^{-8}
μ (Pa)	0	4×10^9	4×10^9

tive lithosphere at the surface, underlain by a thermally conductive boundary layer and an adiabatic zone which together constitute the convective region. The adiabatic zone is assumed isothermal; call this temperature T_c.

Based on the phase diagram and temperature profile, two different internal structures for Ganymede exist (dotted lines in Fig. 2). For $T_c < 251$ K, the entire mantle is frozen. For $T_c > 251$ K, the mantle consists of an uppermost ice layer (ice I), an internal ocean, and a lowermost ice layer (high-pressure ice polymorphs). Specifying T_c specifies both the upper and lower depths of the ocean and the thickness of the uppermost ice layer, i.e., the whole mantle structure.

Assuming an isothermal convection zone below the upper boundary layer should be fine if no melting has occurred. The expected adiabatic temperature increase across the $\sim 10^3$-km-deep ice mantle is about 10 K. Any temperature discontinuities caused by layered convection or phase changes are about 10 K as well. These temperature variations are negligible given our uncertainty in tidal Q.

The assumption of a convecting, isothermal region is not so obvious if internal melting occurs. In absence of convection, tidal heating in ice I would produce a temperature profile following the melting curve. (Darcy's law predicts rapid drainage of the melt water to the ice I–III interface.) This profile is locally *stable* to convection. However, the extreme coldness of the boundary layer should allow strongly non-local convection from above, driving the temperature profile toward a dry adiabat. The convective overturn time is less than the time scale for major temperature changes (discussed later), so relaxation to the dry adiabat seems reasonable. We thus tentatively conclude that convection will occur, an isothermal temperature profile is reasonable, and discrete oceanic and solid ice layers (rather than partially molten regions) constitute the relevant structure when internal melting occurs.

We do not model the detailed evolution of the rock/iron core, since this is unimportant for evolution of the ice mantle.

iv. Heat Source

To determine the heat source from Eq. (1), we need to determine the "effective" Q/k for the whole satellite, which we obtain by assuming Q and k are local quantities and volume averaging their ratio k/Q over the satellite. Although k is not strictly a local quantity, most of the tidal energy dissipation takes place near the surface of the satellite, so the error involved in this formulation should not be large compared with other uncertainties.

The Q of all materials is poorly understood, particularly at tidal frequencies. However, we expect that warming promotes creep in ice and accordingly lowers Q. In warm ice, unlike rock, tidal periods are close to the Maxwell time, so creep is plausible for the anelastic portion of the response. We therefore assume that the Q of ice is determined by the Maxwell model (Ojakangas and Stevenson 1989)

$$Q = \frac{1 + (n\tau_M)^2}{2n\tau_M}, \tag{2}$$

where $n = 1.0 \times 10^{-5}$ sec^{-1} is Ganymede's mean motion and $\tau_M \equiv \eta/\mu$ is the Maxwell time. $\mu = 4 \times 10^9$ Pa is the rigidity of ice, and η is the local ice viscosity. The temperature dependence of η is

$$\eta = \eta_0 \exp\left[A\left(\frac{T_m}{T} - 1\right)\right], \tag{3}$$

where T_m is the local melting temperature, T is the local actual temperature, and η_0 is the melting-point ice viscosity. We treat η_0 as a free parameter, with magnitude 10^{13}–10^{15} Pa sec, the expected range for small grain sizes ($\sim$1 mm; Kirk and Stevenson 1987). We use $A = 26$ (Weertman 1973).

Sample $Q(T)$ curves predicted by Eqs. (2) and (3) are shown in Fig. 3 for values of η_0 from 10^{12} to 10^{15} Pa sec. The low-temperature behavior allows runaways.

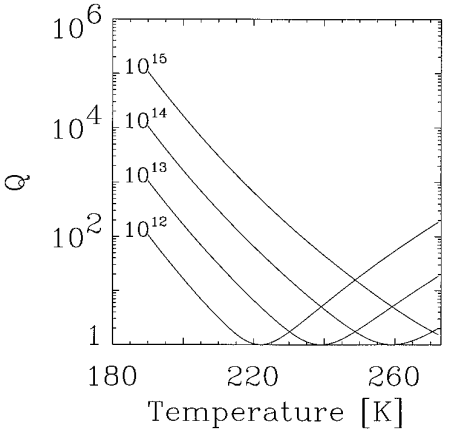

FIG. 3. Ice $Q(T)$ used in thermal model, as determined by the Maxwell model, Eqs. (2) and (3). We use $A = 26$, and show four curves, for η_0 from 10^{12} to 10^{15} Pa sec.

When Ganymede is frozen, we estimate k from the formula for a homogeneous satellite (Munk and MacDonald 1960),

$$k = \frac{3/2}{1 + 19\mu/2\rho g R}, \tag{4}$$

where μ is the shear modulus, ρ is the density, g is surface gravity, and R is the satellite radius. Since the material in the tidal bulge is icy, we use $\rho = 1000$ kg m^{-3} and $\mu = 4 \times 10^9$ Pa, appropriate to ice. This gives $k = 0.14$ for a frozen Ganymede. (We assume k/Q is zero in the rock core.)

When the ocean forms, however, the situation becomes more complicated. Ganymede would then have at least four layers: the outer ice shell, ocean, inner ice shell, and rocky core (which may be further differentiated into silicate and iron layers). The exact deformation of such a body under a variable tidal potential is extremely complex and depends on the rigidity, density, viscosity, and location of each layer. Although this full problem has not been attempted, simpler two-layer problems have been solved by Dermott (1979) and Peale and Cassen (1978); these studies can provide insight. Dermott (1979) showed that for a body consisting of an ocean overlying a solid elastic core, the effective Love number for the solid layer is

$$k = \frac{\frac{3}{2}(1 - \rho_w/\rho)}{1 - \rho_w/\rho + 19\mu(1 - 3\rho_w/5\rho)/2\rho g R_c},$$

where ρ_w is the ocean density, g is gravity at the core–ocean interface, and ρ, μ, and R_c are the core density, rigidity, and radius, respectively. Considering the "core" to be the high-pressure ice phases (which typically have densities 10% greater than that of liquid water at the same pressure), $k \approx 0.04$. Because the ice is near melting temperature, however, viscous creep may be as (or more) important than elastic strain, so the actual tidal deformation is likely to be greater.

Peale and Cassen (1978) explored two-layer models consisting of an elastic outer shell overlying a liquid core, and solved for the deformation in the case where the two layers have equal densities. They found that the effective Love number depends on the shell thickness. For thin shells, the shell's strength is negligible relative to the gravitational force driving the material to an equipotential. The effective Love number is then just 1.5, the value for a fluid planet [obtainable from Eq. (4) using $\mu = 0$]. Thick shells are strong enough to resist the gravitational force and have lower values of k. Peale *et al.* (1979) demonstrated that for Io the transition between the two regimes occurs for shell thicknesses of ~20% the satellite radius, and the transition thickness for Ganymede is probably greater because the rigidity of ice is 10 times less than that of rock. Since Ganymede's ice I layer is only 6% of the satellite radius at ocean formation, we expect that the Love number will discontinuously rise to values near 1.5 when the ocean forms.

Ross and Schubert (1987) explored three-layer models for Europa, consisting of an outer ice shell, ocean, and rocky core, each with different densities and rigidities. They found that the tidal deformation for the thin outer shell is half that predicted by Peale and Cassen's model because the low density and small mass of the outer layers (relative to the core) allow only minimal amplification of the bulge size by self-gravitation. Further, the perturbing effect of the *core's* bulge on the ice shell is small simply because the high rigidity limits the core bulge size. For Ganymede, however, we expect k to be much closer to the Peale and Cassen prediction because the ice mantle is much thicker.

We adopt a highly simplified scheme for calculating k when an ocean exists. We assume that $k = 1.5$ in the ice I layer and continue to use $k = 0.14$ in the lower ice layer; k/Q is taken to be zero in the rock core and ocean, as dissipation is expected to be low there. We then volume average k/Q over the satellite for use in calculating the heat source from Eq. (1). This approach, of course, is not rigorous and may be in error by up to a factor of a few. Despite the lack of precision, however, our approach is justified by the fact that Q has an uncertainty of one to two orders of magnitude. Further, more rigorous calculation would not necessarily improve the accuracy in k. For example, lack of knowledge about salts and other impurities creates uncertainty in the temperature of ocean formation and the density difference between the ocean and ice layers, both of which affect k.

The Maxwell model has the deficiency that it predicts arbitrarily large increases in Q with decreasing temperature. In real ice, dissipation mechanisms other than steady-state creep doubtless prevent this. Accordingly, we terminate the growth of Q/k above 2000, corresponding to $Q \sim 300$ for reasonable k.

We ignore radiogenic heat output and secular cooling or warming of the core. The neglect of radiogenic heat is reasonable if runaways occur over a few $\times 10^8$ years or less.

v. Heat Loss

We use the parameterized convection scheme of Friedson and Stevenson (1983) to calculate the convective heat flux over time in a planet with no plates and strongly temperature-dependent viscosity. Recent theoretical work (Solomatov 1995) supports such scaling, first applied to the icy satellites by Reynolds and Cassen (1979).

The convective flux is given by

$$F_{conv} = c\frac{k_t \Delta T}{d}\mathrm{Ra}^{1/3}, \tag{5}$$

where k_t is thermal conductivity, d is the depth of the convecting layer, ΔT is the temperature drop across the convecting region (equal to the temperature drop across the convective boundary layer in our model, since the adiabat is isothermal and the lower boundary layer is assumed negligible), c is an independent parameter, and the Rayleigh number Ra is given by

$$\mathrm{Ra} \equiv \frac{g\alpha\rho\,\Delta T d^3}{\kappa\eta_{1/2}}. \tag{6}$$

Here g is gravity, α is thermal expansivity, ρ is density, κ is thermal diffusivity, and $\eta_{1/2}$ is the viscosity evaluated at a temperature half-way across the boundary layer. We use $c = 0.1$, which implies a critical Rayleigh number of about 10^3. This choice of c is compatible with Solomatov (1995) to within a factor of 2. We evaluate ΔT by assuming the system adjusts ΔT to maximize F_{conv} for a given T_c (Friedson and Stevenson 1983). This gives

$$\Delta T = 2\{b - [b^2 - T_c^2]^{1/2}\}, \tag{7}$$

where $b \equiv T_c + AT_m/8$. Finally, we find that

$$F_{\mathrm{conv}} = ck_t\left(\frac{g\alpha\rho}{\eta_{1/2}\kappa}\right)^{1/3}(\Delta T)^{4/3}, \tag{8}$$

with ΔT given by (7). The convected flux is independent of the depth of the convecting region, so Eq. (8) applies whether or not Ganymede contains an internal ocean. The scheme assumes, however, that the convecting depth is much greater than the boundary layer thickness. When the ice I layer becomes so thin that Ra < 1000, we assume the heat is conducted out.

vi. Time Evolution of Thermal State

The internal heating rate for the satellite is

$$\frac{dE}{dt} = \frac{21}{2}\left\langle\frac{k}{Q}\right\rangle\frac{GM_J^2R^5ne^2}{a^6} - 4\pi R^2F_{\mathrm{conv}}, \tag{9}$$

where the first term is the tidal dissipation from Eq. (1), with a volume average of k/Q over the satellite.

When Ganymede is completely frozen, the change in T_c over time is related to the change in internal energy E by

$$\frac{dE}{dt} = M_ic_{p_i}\frac{dT_c}{dt}, \tag{10}$$

where M_i is the mass of ice in Ganymede (7.5×10^{22} kg for the frozen state model), and c_{p_i} is the specific heat of ice. When Ganymede contains an ocean, we must consider the latent heat of melting and the different specific heats of liquid water and ice. The change in internal energy over time is then

$$\frac{dE}{dt} = [M_wc_{p_w} + M_ic_{p_i}]\frac{dT_c}{dt} + L\frac{dM_w}{dt}, \tag{11}$$

where M_w is the mass of water, L is the latent heat, and c_{p_w} is the specific heat of liquid water. The first term accounts for warming of the water, the second for warming of the ice, and the third for melting ice. (We assume L is the same for ice I and high-pressure ice; Table I lists the assumed values of L, c_{p_i}, c_{p_w}, and ρ). The rate of growth of the ocean, dM_w/dt, is given by

$$\frac{dM_w}{dt} = \frac{4\pi}{g}\frac{dT_c}{dt}\left[r_u^2\left(\frac{-dp}{dT_m}\right)_1 + r_b^2\left(\frac{dp}{dT_m}\right)_{hp}\right], \tag{12}$$

where T_m is the local melting temperature. r_u is the radius at the ocean–ice I interface, and r_b is the radius at the ocean–high pressure ice interface; the subscripts "1" and "hp" refer to ice I and high-pressure ice. Using equations for the melting curves and hydrostatic equilibrium, we then obtain r_u and r_b as functions of T_c. These relations, plus Eqs. (11) and (12) and the two constraints $M_w = 4\pi\rho(r_u^3 - r_b^3)/3$ and $M_i = 0.5M - M_w$, where M is Ganymede's mass, then constitute a relation between dE/dt and dT_c/dt for a molten Ganymede. The analogous expression for a frozen Ganymede is simply Eq. (10). Therefore Eq. (9) is transformed to an ordinary differential equation in $T_c(t)$, which is coupled to those for $e(t)$ and $a(t)$. We assume that we never melt all of either the ice I or high-pressure ice (i.e., that we always have the latent heat term in the molten state) and neglect the solid–solid latent heats of transition, the largest of which (ice II–III) is roughly 20% of the solid–liquid latent heat.

3. MODEL RESULTS

To perform a simulation, we must specify initial values for ω_1, ω_2, and T_c, as well as the values of the parameters η_0 and c and the Q/k for Io and Europa. We perform runs for two sets of orbital initial states. The first set starts at $\omega_1 = -6.2°$ day^{-1} and $\omega_2 = -2.65°$ day^{-1}, with initial $\omega_1/\omega_2 \approx 2.3$. Thus, we begin the system just short of the $\omega_1/\omega_2 \approx 2$ resonance, so that the system encounters this Laplace-like resonance in the first 10^8 years of evolution. (This allows convenient systematic study of the runaway, since we can better specify T_c just as the resonance is starting. However, the system need not enter resonance so early.) We use $(Q/k)_{Io}/(Q/k)_J = 4 \times 10^{-4}$ and $(Q/k)_{Europa}/(Q/k)_J = 4 \times 10^{-3}$, which yield reasonable values of Q for the expected k for these satellites. [The

low value for $(Q/k)_{\rm Io}$ is required for capture into $\omega_1/\omega_2 \approx 2$ (Showman and Malhotra 1997).]

For the second set, we start at $\omega_1 = -4.7°$ day^{-1} and $\omega_2 = -8.0°$ day^{-1}, so that $\omega_1/\omega_2 \approx 0.6$. In this case, the system encounters the $\omega_1/\omega_2 = 1/2$ resonance. We use the same $(Q/k)_{\rm Europa}$ as above, but use $(Q/k)_{\rm Io}/(Q/k)_{\rm J} = 1.1 \times 10^{-3}$. This is the value Io would have at present if its present eccentricity were constant in time. Both resonances can lead to the Laplace resonance and are therefore plausible paths to the current state (Showman and Malhotra 1997, Malhotra 1991).

In each of these two sets of runs, we used $\eta_0 = 10^{13}$, 10^{14}, and 10^{15} Pa sec, and a range of values for initial $T_{\rm c}$.

Three general types of model behavior were found, exemplified by the three runs displayed in Figs. 4, 5, and 6. All three runs passed through the $\omega_1/\omega_2 = 2$ resonance, followed by capture into the Laplace resonance; they differed only in the initial temperature $T_{\rm c}$ of Ganymede. In each of the figures, (a) shows the time evolution of Ganymede's eccentricity, (b) shows Ganymede's ice mantle temperature $T_{\rm c}$, and (c) shows Ganymede's effective Q/k. (Because we have assumed an isothermal adiabat, the entire state of the mantle at a particular time corresponds to a single value of $T_{\rm c}$.) In all panels, the time axes are the same, $t = 0$ to 4×10^9 years.

In Fig. 4, Ganymede starts warm, with initial $T_c = 271$ K, implying existence of a large internal ocean. Q/k thus starts low, so the resonance is never able to pump the eccentricity to a high value: the maximum eccentricity attained is 0.002 (Fig. 4a). Thus, runaway is not possible. From Fig. 4b, the temperature can be seen to reach a steady state (at ~2 Ga) in which convective cooling balances dissipative heating. (The ice I layer is 80 km thick and the ocean is several hundred kilometers deep at this time.) At 2.6×10^9 years, $(Q/k)_{\rm Io}/(Q/k)_{\rm J}$ (an imposed free parameter) is increased by a factor of 6 to 1.9×10^{-3}, disrupting the $\omega_1/\omega_2 \approx 2$ resonance and leading to capture into the Laplace resonance (see Showman and Malhotra 1997). Thereafter, the satellite cools monotonically. The kink in $T_{\rm c}$ at 3.6 Ga corresponds to freezing of the ocean, at which point latent heat buffering ceases. The mean tidal heating rate during the resonance was roughly 10^{12} W.

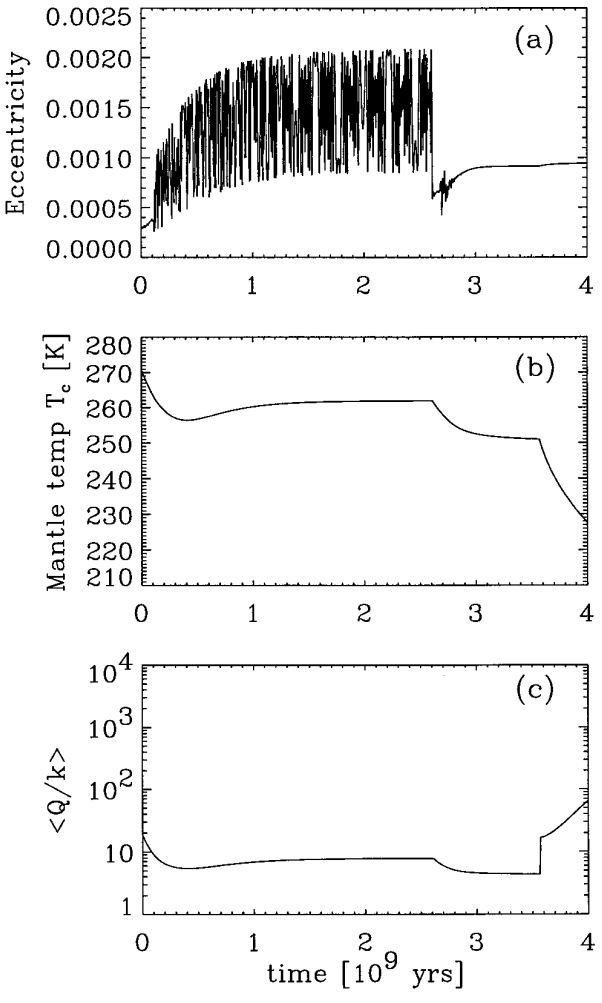

FIG. 4. Results of a run from the Ganymede coupled orbital–thermal model. (a) Ganymede's eccentricity, (b) Ganymede's mantle temperature $T_{\rm c}$, and (c) Ganymede's effective Q/k versus time for 4 byr of evolution (the time axes in all three plots are the same). In this run the system passes through the $\omega_1/\omega_2 \approx 2$ resonance before capture into the Laplace resonance at 2.6 Ga. The final state in this run thus resembles that of the modern state. No radiogenic heating is included. In this run, Ganymede has begun warm ($T_{\rm c} = 271$ K), and no runaway occurs.

In Fig. 5, the satellite starts cold and frozen, with $T_{\rm c} = 170$ K. Q/k is high, and tidal energy dissipation is small. The increase in dissipation caused by increasing e is not enough to change the temperature significantly during the resonance: the internal temperature is nearly constant throughout the evolution. Thus, no runaway has occurred. At 2.6×10^9 years, the system is again disrupted into the Laplace resonance.

In Fig. 6, we start Ganymede at an intermediate temperature of 183 K. Q/k starts high enough to allow the eccentricity to rise, but low enough that the increase in eccentricity to 0.02 causes some warming. Eventually Q/k begins to decrease. The warming then accelerates, and a runaway occurs. The temperature warms by 65 K, and an ocean several hundred kilometers deep forms. In this example, about half of the temperature increase occurs in 10^7 years. In Fig. 6 the $\omega_1/\omega_2 \approx 2$ resonance continues to exist after the thermal runaway has occurred; the resonance does not end until 2.6×10^9 years (again triggered by an increase in $Q_{\rm Io}$), at which time the Laplace resonance is established. The $\omega_1/\omega_2 \approx 2$ resonance is thus stable against large decreases in the Q/k of Ganymede; this is true of $\omega_1/\omega_2 \approx 3/2$ and 1/2 as well. The minimum ice I thickness (which occurs just before 2.6 Ga) is ~80 km. Note that the eccen-

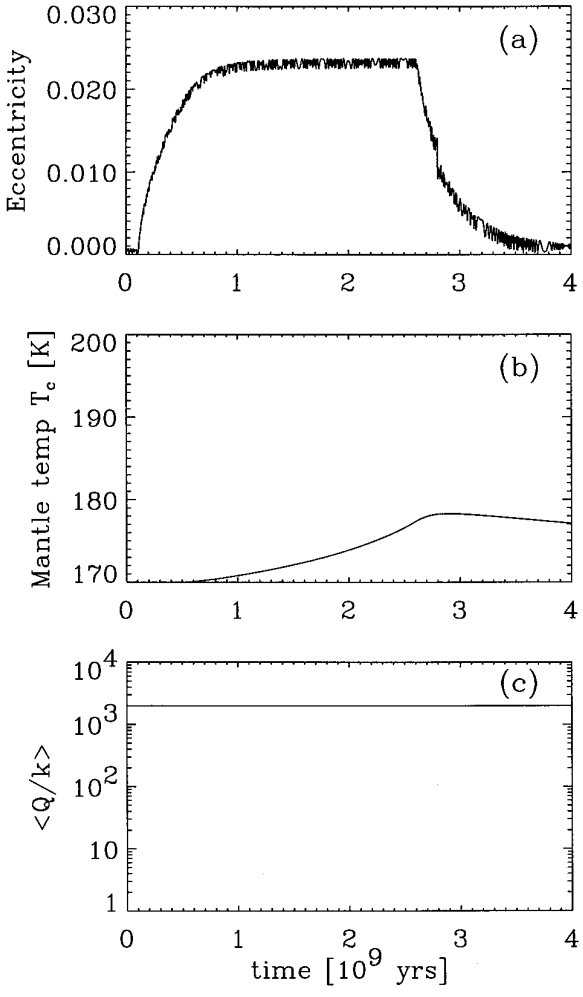

FIG. 5. Same as Fig. 4, but for a colder initial mantle temperature of T_c = 170 K. In this run, Ganymede has begun too cold, and no runaway occurs.

tricity after the runaway is comparable to that in Fig. 4, because Q/k is roughly the same.

The runaway magnitude (quantified by the temperature rise) and the runaway time scale both vary with initial T_c. Figure 7 summarizes our results for two Laplace-like resonances, $\omega_1/\omega_2 \approx 2$ (solid dots) and $\omega_1/\omega_2 \approx 1/2$ (open squares), in runs with a choice of $\eta_0 = 10^{15}$ Pa sec. The time scales shown are the times needed for approximately two-thirds of the temperature rise to take place. Runaways can occur in the $\omega_1/\omega_2 \approx 3/2$ resonance, as well; these are slightly weaker than those with $\omega_1/\omega_2 \approx 2$.

Several features are evident. First, the largest runaway causes about 70 K warming, and a continuum of smaller runaways exist. Second, the shortest runaway occurs in just over 10^7 years, and a continuum of slower runaways exist. Third, time scale is inversely correlated with the magnitude: the shortest runaways are also the largest. The thickness of the ice I layer is roughly 130 km immediately after the largest runaways.

We performed runs using $\eta_0 = 10^{13}$ Pa sec and $\eta_0 = 10^{14}$ Pa sec as well. Qualitatively, the results are very similar to those shown in Fig. 7, except that the curves are shifted to lower temperatures. In other words, the strongest runaways start at ~170 K for $\eta_0 = 10^{14}$ Pa sec and ~150 K for $\eta_0 = 10^{13}$ Pa sec, as compared with 190 K for $\eta_0 = 10^{15}$ Pa sec. Therefore, the models with lower melting-point viscosity are less likely to produce oceans.

Interestingly, the temperature continues to rise after a runaway has occurred in the $\omega_1/\omega_2 \approx 2$ or 3/2 resonance, eventually reaching a steady state in which surface cooling balances dissipative warming. The minimum ice I thickness therefore often occurs several hundred million years after the runaway. The reason is that for c = 0.1, the steady-

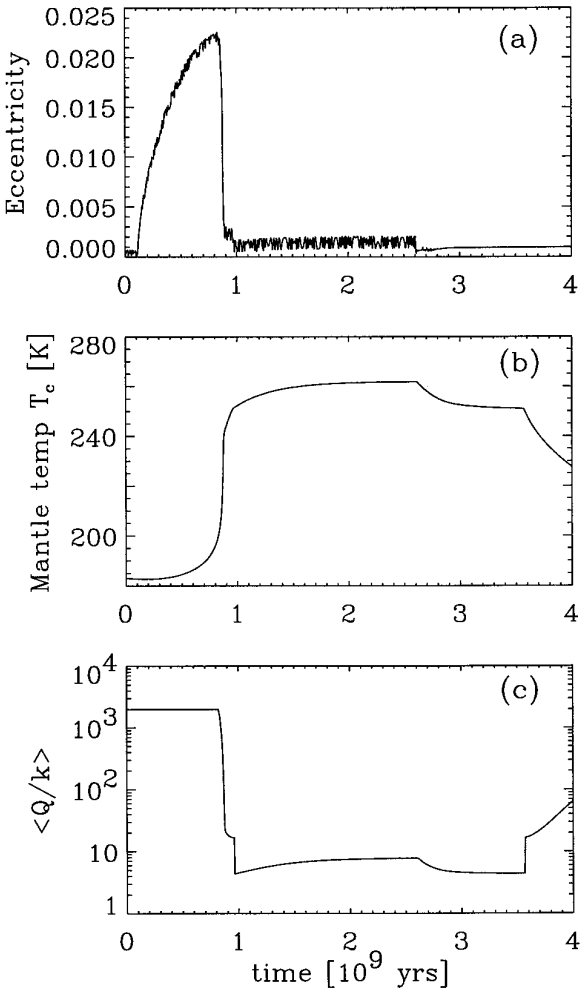

FIG. 6. Same as Fig. 4, but for an intermediate starting temperature of 183 K. In this run, Ganymede's temperature is just right, and a large runaway occurs: Ganymede's mantle warms by ~65 K and a large ocean forms in just ~10^7 years.

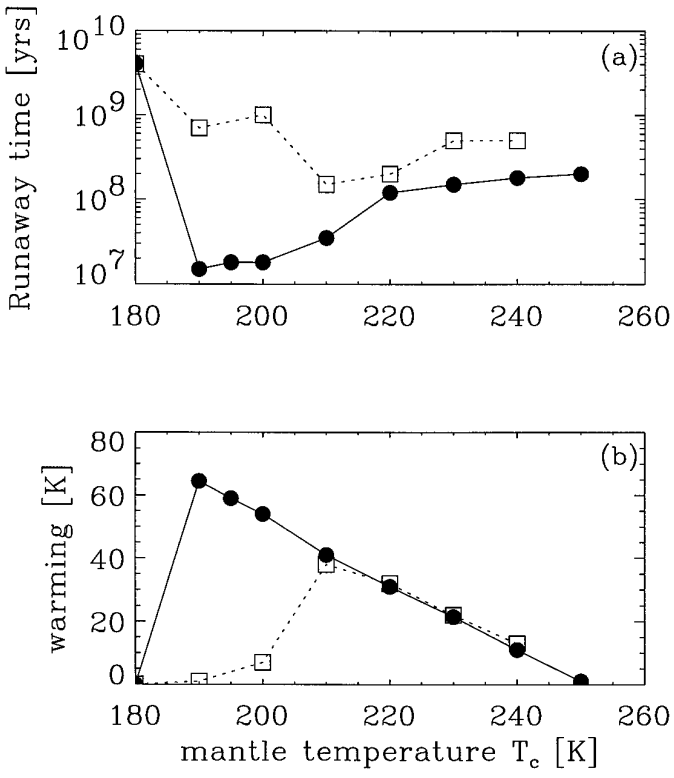

FIG. 7. Summary of results on thermal runaways from coupled orbital–thermal model. (a) Time over which runaway occurs and (b) warming occurring during a runaway, as a function of Ganymede's mantle temperature T_c at the onset of resonance. Each circle or square represents the results of a model run. Filled circles represent runs passing through $\omega_1/\omega_2 \approx 2$; open squares correspond to runs passing through $\omega_1/\omega_2 \approx 1/2$. All runs use the Maxwell model for $Q(T)$, with the constraint that Q/k not exceed 2000. The runs shown use $\eta_0 = 10^{15}$ Pa sec, $c = 0.1$, and $Q_J = 3 \times 10^5$.

state mantle temperature (for the high tidal dissipation rate in $\omega_1/\omega_2 \approx 3/2$ or 2) is at least 70 K above the temperature needed to initiate large runaways. Since runaways produce less than 70 K warming, the temperature immediately following runaway is colder than the steady-state value. If $c \geq$ several $\times 10^{-1}$, however, cooling (rather than warming) always follows the runaway, implying that the ice I layer reaches its minimum thickness during runaway. [Assuming values of c greater than 0.1 is equivalent to assuming that ice is softer at convective time scales than tidal flexing time scales; see Eqs. (5) and (6).]

We assumed $Q_J = 3 \times 10^5$ in all our runs. The runaways would be weaker for larger Q_J and vice versa. For example, if Q_J were near its time-averaged lower limit of a few $\times 10^4$, Ganymede's eccentricity would rise to 0.04 rather than 0.02 before a large runaway (see Fig. 7 in Showman and Malhotra 1997). The strongest possible runaways would then be four times more energetic than those displayed in Figs. 6 and 7, and the steady-state ice I thicknesses would be smaller.

The magnitude of tidal flexing at the surface is important for models of resurfacing. According to the models discussed here, $e \sim 0.02$ before a runaway and about 0.001 afterward (Fig. 6). Conversely, $k \approx 0.14$ before and 1.5 afterward. These conditions imply a tidal strain amplitude of a few $\times 10^{-6}$ or less both before and after runaway. However, during a runaway, the ice shell decouples (implying $k = 1.5$) while the eccentricity is still high. The maximum achievable eccentricity at decoupling is 0.01 for the $\omega_1/\omega_2 \approx 2$ resonance. This yields a strain amplitude of 10^{-5} over a period of 10^7 years.

The results in Fig. 7 show that large runaways cannot occur unless the mantle temperature is below 200 K at the onset of resonance. However, radiogenic and accretional heating may prevent cooling to such temperatures. We now consider the question of whether Ganymede can cool to 200 K before resonant eccentricity pumping begins. To do this, we must know when resonant heating began.

Traditional crater dating techniques yield ages for Ganymede's grooved terrain of ~3.5 byr (Shoemaker and Wolfe 1982). This age for the cratered terrain was obtained using a modern cratering rate of 2.3×10^{-14} km^{-2} year^{-1} for 10-km-diameter craters (Shoemaker and Wolfe 1982), and assuming that the impact rate of comets doubled 0.5 byr ago (as indicated in the lunar and terrestrial cratering history). However, recently revised estimates yield 1.1×10^{-13} km^{-2} year^{-1} for the modern 10-km crater production rate (E. M. Shoemaker, personal communication, 1995), which suggest ages for the grooved terrain of a billion years or less. The uncertainty in these estimates means that we cannot as yet place a constraint on the time at which tidal heating began.

We consider the most generous scenario, in which resonant heating begins late in solar system history. We therefore wish to determine whether Ganymede can cool to 200 K over solar system history.

We start Ganymede differentiated, with initial $T_c = 270$ K 4.6 byr ago, and use the Ganymede model with no tidal dissipation (i.e., zero eccentricity). Such a warm starting temperature is suggested by plausible accretion scenarios (McKinnon and Parmentier 1986). We include a core model to account for radiogenic heating since this heat source substantially affects the cooling rate. We run the model for two cases: (1) using carbonaceous chondritic radionuclide abundances for the core rock, and assuming that all radionuclides are contained in the core; (2) using carbonaceous chondritic abundances, but assuming 30% of the radionuclides were leached into the ocean. If Ganymede rock were ordinary chondritic (i.e., with a K/U ratio close to that of the terrestrial mantle), the radiogenic output would be intermediate between the carbonaceous chondritic cases and that with no radionuclides, since ordi-

nary chondrite is substantially depleted in ^{40}K relative to carbonaceous chondrite.

We use the core model of Kirk and Stevenson (1987). The model assumes carbonaceous chondritic abundances for ^{40}K, ^{232}Th, ^{235}U, and ^{238}U. The core initially starts at 270 K, the same as the ice mantle, and gradually warms as the radionuclides decay. Initially, heat is conducted into the ice mantle across a boundary layer of thickness $(\kappa_c t)^{1/2}$, where κ_c is the thermal diffusivity of the core rock. Once the core Rayleigh number reaches 10^3, convection begins. In this regime, the model assumes the core "self-regulates," so that the power released to the ice equals the instantaneous radiogenic power production. We use a core rock melting-point viscosity of 1.7×10^{16} Pa sec rather than 1.7×10^{13} Pa sec as used by Kirk and Stevenson (1987).

In Fig. 8 we show T_c over time resulting from the above model, using $k_t = 4.1$ W m^{-1} K^{-1} and $c = 0.1$ for the ice mantle model. Figures 8a and 8b correspond to cases 1 and 2 above, and Fig. 8c corresponds to no radiogenic heating. In each case we show curves for four separate runs, for $\eta_0 = 10^{12} - 10^{15}$ Pa sec. With no radiogenic heating, T_c plummets below 200 K for all four runs, so runaway seems possible if resonance capture were to occur. However, Figs. 8a and 8b show that radiogenic heating prevents the mantle from cooling to 200 K; for $\eta_0 = 10^{15}$ Pa sec, the ocean never freezes. The implication is that large runaways are unlikely if Ganymede's core rock contains carbonaceous chondritic radionuclide abundances, although small runaways (initiated from $T_c \sim 220$–230 K) could still occur.

The failure of our model to predict large, ocean-forming global runaways should be taken seriously, and may mean that such runaways are impossible. However, our model contains several major uncertainties. First, our formulation of Q is particularly suspect. We equated viscosities at tidal flexing (1-week) and convective overturn (10^7-year) time scales. If ice were four to five orders of magnitude softer at convective time scales than at tidal time scales, large runaways would be possible. Alternatively, if additional dissipation mechanisms besides viscous creep cause $Q(T)$ to be strongly temperature dependent near melting, reasonable values of η_0 (10^{12} Pa sec) at convective time scales could allow large runaways. Second, although the work of Solomatov (1995) strengthens our parameterization of convection in the ice mantle, we stress that the formulation is still not rigorous and is subject to uncertainty. Finally, a major depletion of radionuclides in Ganymede's rocky portion would allow sufficient cooling for large runaways to occur, although such depletion is unlikely.

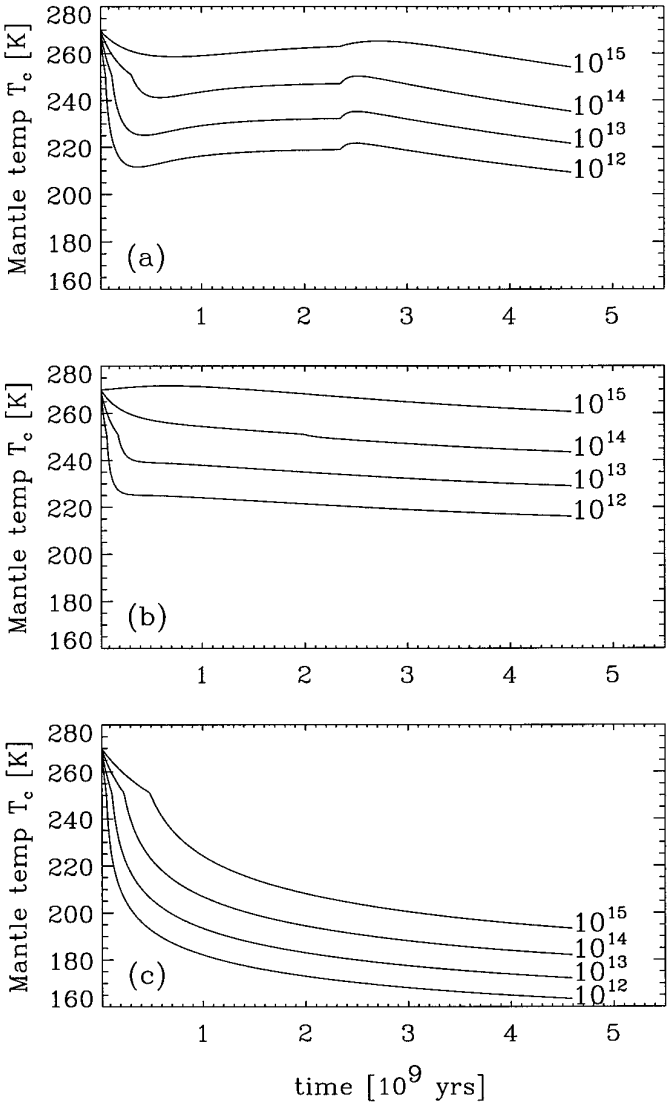

FIG. 8. Ganymede's mantle temperature T_c over 4.6 byr, assuming no resonant eccentricity pumping. Uses Ganymede model from Section 2 with the rock core model of Kirk and Stevenson (1987). (a) Evolution for carbonaceous chondritic radionuclide abundances for rock core, and assuming 100% of radionuclides remain in core, (b) same, but assuming 30% of nuclides have been leached into the ocean and 70% remain in core. (c) No radiogenic heating. Each panel shows evolution for four model runs, with values of η_0 from 10^{12} to 10^{15} Pa sec. With radiogenic heating, the temperature never drops below 200 K. Since large runaways require such low temperatures, they may be impossible.

4. EFFECTS OF RUNAWAY: GLOBAL EXPANSION

The observation that bright terrain edges are sharp and linear strongly suggests that bright terrain formed in a global system of graben. This interpretation, as well as other geologic features (Parmentier *et al.* 1982) suggest global expansion. Ganymede thermal models (Schubert *et al.* 1981, McKinnon and Parmentier 1986) generally predict extensive or complete differentiation early in solar system history. Therefore, any global expansion and lithospheric fracture accompanying differentiation are probably not as-

sociated with grooved terrain formation, as suggested by some authors (Squyres 1980).

Although our model does not predict large runaways, the uncertainties of our model, the lack of other processes capable of causing global expansion, and the success of our model in predicting small runaways warrant consideration of the effects of runaway. The warming and phase changes during global runaway could cause the inferred expansion.

4.1. *Expansion Caused by Melting*

Here we consider the expansion undergone by Ganymede in passing from a warm, frozen state (as in Fig. 1b) to a state with an internal ocean (as in Fig. 1c, 1d, or 1e). We calculate only the volume changes that accompany the phase change of ice into liquid water. (Thermal expansion is considered in the next section.) In addition, we neglect the small volume change associated with conversion of ices I and V to ice III as the temperature warms. Under these assumptions, we need not specify the details of temperature with depth in the ice. (However, we will need the oceanic temperature profile.)

We take as initial state a frozen, differentiated Ganymede consisting of a rock core overlain by a pure water ice mantle of ices I, III, V, and VI, corresponding to a mantle temperature of ~240–250 K. (At these temperatures, Ganymede cannot contain any ice VII or VIII for reasonable core densities.) We characterize this initial state by specifying pressure with depth. To do this we specify gravity as a function of depth and integrate the hydrostatic equation down from the surface, assuming incompressible ice phases with densities of 0.92, 1.16, 1.27, and 1.31 g cm^{-3} for ices I, III, V, and VI, respectively. The expressions are valid only as long as the core radius is smaller than the radius in question. With this caveat, however, the expressions are independent of core density (and, therefore, radius). We assume $p(r)$ does not change during the melting process; r is the local radius from Ganymede's center.

Let the local volume change per mass (m^3 kg^{-1}) from ice i (where i = 1, 3, 5, or 6 for ice I, III, V, or VI, respectively) to liquid water be $\Delta v_{il}(p)$. We assume Δv_{il} is linear with pressure and interpolate between values at triple points, using data from Fletcher (1970). Using our $p(r)$ relations, we then obtain relations for $\Delta v_{il}(r)$. We next integrate $\Delta v_{il}(r)$ over the appropriate spherical shell to obtain the volume change of the shell, ΔV_{il}, when that shell has been converted from ice to liquid. The total volume change is obtained by summing the volume changes of the individual shells. To calculate the total volume change, we must know the thickness of the ocean as a function of the depth of the ocean–ice I interface.

For a given pressure at the upper surface of the ocean, we can find the pressure at the lower surface by locating the point at which the oceanic adiabat $dT/dp = \alpha T/\rho_w c_p$ crosses the high-pressure ice melting curve. The thermal expansivity, α, changes by a factor of several along such an adiabat, while the temperature, T, the density of liquid water, ρ_w, and the specific heat, c_p, change by only 10–20%. We thus approximate the latter three as constant, with values 270 K, 1100 kg m^{-3}, and 3900 J kg^{-1} K^{-1} (typical of conditions at a few kilobar), and take α to be piecewise linear with pressure along the adiabat, with fits to data from Dorsey (1940, pp. 232–233) and Weast (1987). We then solve to obtain $T(p)$ along the adiabat (for a given pressure at the ice I–ocean interface). We equate this temperature to the melting curve of ice III, V, or VI, and solve for the ocean thickness as a function of the depth of the ice I–ocean interface. More detailed calculations, performed using linear fits to c_p and ρ_w and letting T vary, give relations in good agreement with those described above.

We modify the expressions for ΔV_{5l} and ΔV_{6l} because of the rock core: once pressure at the ocean–high-pressure ice interface exceeds the pressure at the rock core–ice mantle boundary, no more melting of high-pressure ice can occur, and any continued melting of ice I leads only to satellite contraction, not expansion. This affects the way we sum the volume changes ΔV_{il}.

Some data suggest that the room-pressure regime of negative thermal expansivity from 0 to 4°C exists also at higher pressure, perhaps following the ice I melting curve, although other data suggest that high-pressure thermal expansivity is positive everywhere (Dorsey 1940, p. 230). Such a region of negative thermal expansivity (which might constitute the uppermost 10^2 m of ocean for fluxes of 10^{-2} W m^{-2}) would be stable against convection, and would thus act as a thermally conductive boundary layer, increasing interior temperatures for a given external temperature. For a given volume of ice I melted, the volume of high-pressure ice melted would be greater than that if α were positive everywhere. We considered two cases: assuming (1) thermal expansivity is positive everywhere, so that the adiabat strikes the ice I melting curve directly; (2) at any pressure along the ice I melting curve, the region between the melting temperature T_m and T_m + 4 K is considered to have negative expansivity (equivalent to assuming an oceanic adiabat 4 K warmer than before for a given pressure at the ocean's upper surface).

We plot the final results in Fig. 9. There, we show the net satellite volume change from our frozen reference state as a function of ice I layer thickness. (Specifying the ice I thickness determines the ocean's depth and the entire satellite structure, for a given rock core size. The core size is uniquely specified by the core density.) We show the results for both assumptions about thermal expansivity and for core densities of ρ_c = 2.5, 3.0, and 3.5 g cm^{-3} in Figs. 9a, 9b, and 9c, respectively. Expansion is always predicted. Simple calculation shows that if gravity and density are

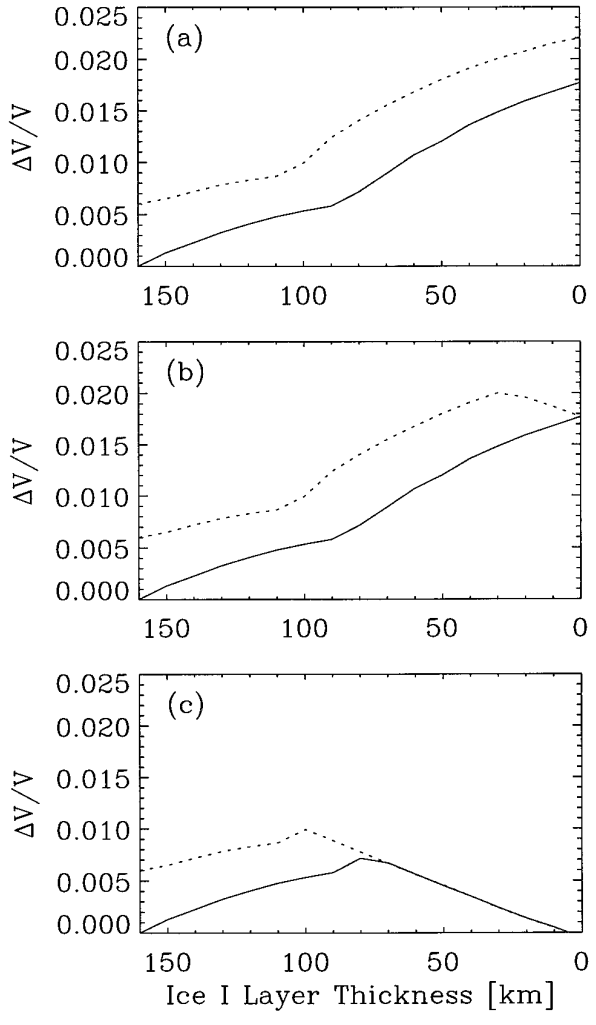

FIG. 9. Fractional volume expansion occurring in Ganymede because of internal melting, shown as a function of ice I layer thickness, for three core densities: (a) $\rho_c = 3.5$ g cm^{-3}, (b) $\rho_c = 3.0$ g cm^{-3}, (c) $\rho_c = 2.5$ g cm^{-3}. The expansion is that relative to a frozen reference state, for which the ice I layer is 160 km thick. Each panel displays the results for two cases: (1) assuming thermal expansivity is positive everywhere (solid curve), and (2) assuming a 4 K region of negative expansivity follows the ice I melting curve (dotted curve), which implies a 4 K boundary layer at the top of the ocean. The expansions shown, of order 1–2%, are those that might accompany a large thermal runaway.

constant with depth, if the area of an infinitesimal spherical shell is constant with depth (i.e., if a "plane-parallel" Ganymede is assumed), if the entropies of transition from ices I, III, V, and VI to liquid are assumed to be equal, and if the oceanic adiabat is isothermal, then the volume change on melting is exactly zero. Relaxing these assumptions leads to a residual volume change. Most importantly, using a realistic adiabat allows more high-pressure ice to melt for a given volume of ice I melted than for an isothermal adiabat, leading to net expansion.

For each case, as expected, $\Delta V/V$ is greater when we allow the region of negative α than when α is positive everywhere. For a small core, $\rho_c = 3.5$ g cm^{-3}, the expansion peaks at ~2% for complete melting of the ice I layer. For a large core ($\rho_c = 2.5$ g cm^{-3}), however, all the ice VI is gone after only about half of the ice I melts. The expansion thus peaks at ~1% and declines with further melting of ice I. In the positive α cases, expansion begins at $\Delta V/V \approx 0.006$. This is because no melting of ice I occurs (except for the 10^2-m boundary layer) until all the ice III and part of the ice V is melted.

Our results differ from those of Squyres (1980) by a factor of several, and have a different dependence on core density. In his pioneering work on the Ganymede–Callisto dichotomy, Squyres calculated that for $\rho_c = 3.5$ g cm^{-3} no expansion occurs on melting, and for $\rho_c = 2.5$ g cm^{-3} volume expansion is 2.2% if the final ice I thickness is 100 km (three to four times larger than our calculated expansion for the same final ice I thickness). However, this dependence on core density cannot be correct for a differentiated Ganymede with pure water ice mantle. As long as the core is small enough that some high-pressure ice remains, the expansion from a frozen reference state is *independent* of core density. A 100-km-thick ice I layer implies that the radius at the ocean bottom is greater than the core radius for $\rho_c \geq 2.5$ g cm^{-3}. Thus, for relevant core densities, $\Delta V/V$ should be constant with respect to ρ_c for the 100-km final ice I thickness chosen by Squyres (1980).

4.2. *Expansion Caused by Solid–Solid Phase Changes and Warming*

We now calculate the expansion when Ganymede passes from a cold frozen state to a warm frozen state. We assume a differentiated Ganymede with a pure water ice mantle of ices I, II, and VI, at a temperature of ~200 K. We take as final state a Ganymede with ices I, III, V, and VI and assume the same $p(r)$ relations as before.

During the transition, ice II changes to ices I, III, and V. Conversion to ices I and III causes expansion, while conversion to ice V causes contraction. Assuming that the local volume change per mass from ice II to ice I, III, or V is independent of pressure (with values of the triple points taken from Fletcher 1970), we find that the expansion largely cancels the contraction. The net expansion/contraction is of magnitude 0.001 or less, which is negligible.

The thermal expansivity of ice I at 250 K is 1.5×10^{-4} K^{-1}; we adopt this value for all the ice polymorphs. Since essentially all of Ganymede's ice mantle will warm during a runaway, and since Ganymede is roughly half ice by mass, the fractional satellite expansion during a runaway is $\sim 7 \times 10^{-5}$/K of warming. This gives $\Delta V/V \approx 0.005$ for the largest runaways described in Section 3.

TABLE II
Ice Flow Law Parameters for $T < 195$ K

Reference	B	m	Q^*
Kirby *et al.* (1987)	1.0×10^{-31} Pa$^{-4.7}$ sec^{-1}	4.7	36 kJ mole^{-1}
Durham *et al.* (1992)	1.0×10^{-35} Pa$^{-5.6}$ sec^{-1}	5.6	43 kJ mole^{-1}

5. LITHOSPHERIC STRESS

In this section, we calculate the lithospheric stress induced by satellite expansion during a runaway. We assume a steady-state strain rate relation of the form

$$\dot{\varepsilon} = \frac{\sigma}{\eta} + B\sigma^{\mathrm{m}} \exp\left(-\frac{Q^* + pV^*}{RT}\right), \tag{13}$$

where σ is stress, η is the volume diffusion (Newtonian) viscosity, given by Eq. (3), p is confining pressure, Q^* is activation energy, and V^* is activation volume. B and m are empirical constants; R is the gas constant. Laboratory experiments suggest $m \sim 3$–5 (e.g., Kirby *et al.* 1987). Note that we neglected the second term in calculating tidal Q and convective heat flow.

Ganymede's surface temperature is roughly 130 K, so for thermal gradients of order 5 K km^{-1}, we are interested in temperatures below 200 K if we consider the uppermost 10 km of lithosphere. This corresponds to confining pressures less than 10^2 bars. Recent experiments on the rheology of ice at these temperatures and 500 bars confining pressure have been performed by two groups (Kirby *et al.* 1987, Durham *et al.* 1983, 1992), who obtain different values for B, m, and Q^*. We use both sets of results (listed in Table II) in our stress calculations and take $\eta_0 = 10^{14}$ Pa sec. Although we are interested in pressures lower than those of the experiments, the pV^* term is negligible for experimentally determined values of V^* (Durham *et al.* 1983, Jones and Chew 1983).

To find stress as a function of lithospheric temperature, we use the strain rate of Eq. (13) in a generalized version of the Maxwell viscoelastic equation,

$$\frac{\dot{\sigma}}{\mu} + \frac{\sigma}{\eta} + B\sigma^{\mathrm{m}} \exp\left(\frac{-Q^*}{RT}\right) = \dot{\varepsilon}, \tag{14}$$

where μ is the shear modulus and the dot denotes time derivative. We have simply taken the steady-state creep rate and added to it the elastic strain rate to give the total strain rate. Because global expansion does not depend on lithospheric stress, we can independently specify $\dot{\varepsilon}$ as a function of time and solve the differential equation to find the maximum value of stress at a given temperature. We take $\dot{\varepsilon}$ to have a Gaussian form

$$\dot{\varepsilon} = \left(\frac{\Delta V}{3V}\right) \frac{1}{\tau\sqrt{\pi}} \exp\left(-\frac{(t - 3\tau)^2}{\tau^2}\right), \tag{15}$$

where t is time, τ is the characteristic expansion time scale, and $\Delta V/V$ is the fractional volume expansion. Then, at any time t, the cumulative linear strain is $(\Delta V/3V)\ \mathrm{erf}(t/\tau)$, which is just $\Delta V/3V$ as $t \to \infty$. We solve Eq. (14) starting at $t = 0$ (three standard deviations away from the peak), and use $\Delta V/V = 0.02$.

Figure 10 shows the peak stress as a function of depth using the flow parameters of Durham *et al.* (1992), for expansion time scales of $\tau = 10^6$ to 10^8 years. Figures 10a, 10b, 10c show the results for surface temperatures of 130, 110, and 90 K, respectively. (The latter may be relevant since the Sun was less luminous several billion years ago.) We assume a thermal gradient of 5 K km^{-1}. The different curves in each panel correspond to stresses attained for different expansion time scales, marked in the figure. We also show the hydrostatic pressure with depth (dotted lines); the intersection between this curve and $\sigma(z)$ depicts the maximum depth of open fracture for ice with zero strength [the actual tensile strength may be ~10–30 bars (Kirk and Stevenson 1987, Squyres 1982)]. These results show that open cracks could occur to a depth of a few kilometers and might cause the inferred graben. Cracks could conceivably propagate to a greater depth.

Stresses calculated using Kirby and co-workers' rheology are at most 30% lower than those calculated using Durham and colleagues' (1992) data. Increasing the value of B by an order of magnitude to account for the possibility of particulate contamination in the ice, as suggested by Durham *et al.* (1992), has only a minor effect on the results.

6. CONCLUSIONS

The mean frictional heating Ganymede undergoes within the eccentricity pumping Laplace-like resonances is generally quite low, and exceeds primordial radiogenic heating only for particular choices of poorly known parameters (e.g., Q_{J}, the tidal Q of Jupiter). It is therefore unclear how resurfacing would occur on Ganymede but not Callisto, since at first glance resonance passage appears to have only a secondary effect on Ganymede's thermal evolution. However, frictional heating is qualitatively different than radiogenic heating because it can depend on the thermal state. Non-linear effects are therefore possible wherein the heating rate varies in time, far exceeding radiogenic heating during short time intervals. This would place Ganymede's thermal history in a qualitatively different regime than Callisto's and might allow resurfacing. Our

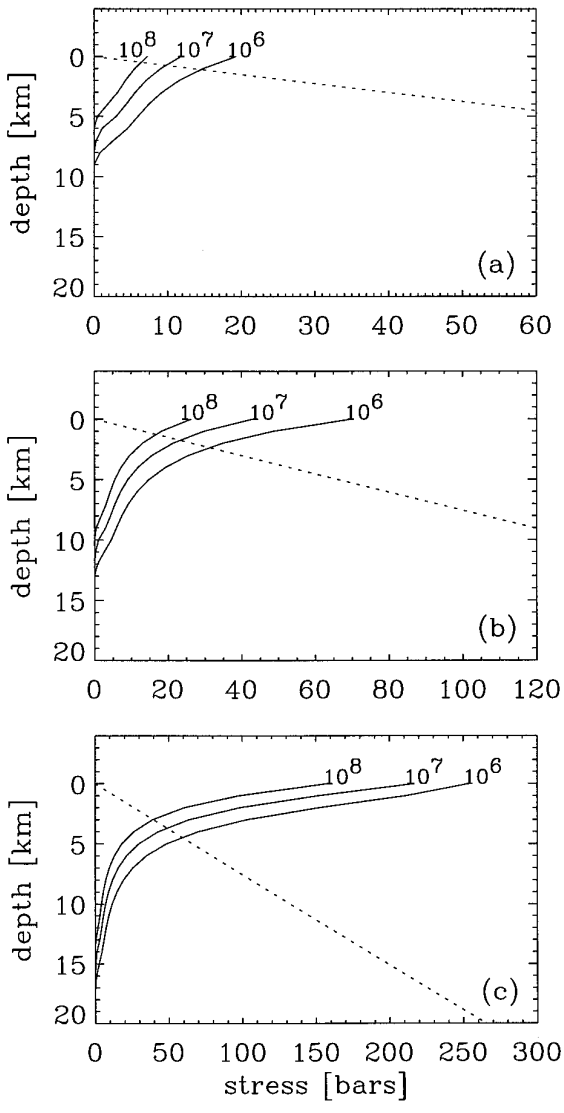

FIG. 10. Lithospheric stress versus depth occurring for a volume expansion of 2%, using flow parameters of Durham *et al.* (1992), for the expansion times shown in the plots (years). Assumes $dT/dz = 5$ K km^{-1}. Dotted line is hydrostatic pressure. (a) Surface $T = 130$ K, (b) surface $T = 110$ K, (c) surface $T = 90$ K. Note the different horizontal scales. The stresses shown imply cracking to several kilometers depth during a large thermal runaway.

goal has been to explore this phenomenon under "garden-variety" scenarios in which mean tidal heating is below primordial radiogenic heating. We have extended the models of Malhotra (1991) and Showman and Malhotra (1997) for the orbital evolution of the Galilean satellites to include the thermal evolution of Ganymede. For plausible dependence of tidal Q/k on temperature, thermal runaway events can occur in Ganymede during tidal evolution preceding capture into the Laplace resonance. We have explored such runaways for the $\omega_1/\omega_2 = 1/2$, 3/2, and 2 Laplace-like resonances. Runaway time scale and magnitude vary sensitively on the details of the model for $Q(T)$ and the initial temperature, but a wide range of initial conditions can lead to runaway.

Convective cooling over billion year time scales appears insufficient for Ganymede to reach the ~200 K temperatures needed for large runaways, for carbonaceous chondritic radionuclide abundances in Ganymede's rock. Thus, large runaways cannot occur if our model is correct, but small runaways are possible. (Scenarios in which Ganymede is "too cold" for runaway—depicted in Fig. 5—are therefore also ruled out.) Different parameterizations of tidal Q or convective heat flow could allow large runaways.

Massive melting of Ganymede leads to a fractional volume expansion of 1–2%, assuming reasonable core densities. Thermal expansion for the largest runaways is 0.5%. Additional expansion may occur if differentiation is not complete when the runaway begins. The total expansion expected *if* a large runaway can occur is thus ~2–3%. Surface stresses caused by 2% expansion over 10^6–10^8 years are $\sim 10^2$ bars at the surface, and drop to a few bars at several kilometers depth.

There are several possible mechanisms for resurfacing. Liquid water could be pumped to the surface by tidal flexing or thermal expansion stresses; such water might derive from a global ocean or from melting of near-surface lithospheric ice during local thermal runaways. These mechanisms are far more likely with large tidal flexing, and probably are not viable unless the tidal strain amplitude exceeds 10^{-5} (Showman and Stevenson 1996). Alternatively, slush or soft ice diapirs may buoyantly rise to the surface; this mechanism requires existence of lithospheric conduits through which the diapirs can rise. This is why the global runaway scenario is so attractive: for our thermal model, the strain amplitude exceeds 10^{-5} only during large global runaways; further, the rapid global expansion occurring during runaways allows cracking, providing conduits for slush and explaining the inferred set of graben. (*Rapid* expansion is required because otherwise the strain would be accommodated by viscous creep rather than cracking.) Thus, resurfacing seems problematic if a large global runaway cannot occur.

Even if Ganymede can cool to the appropriate temperatures for runaway, our model cannot predict the time at which the runaway (and presumably resurfacing) occurred. We can easily produce a runaway at any time during solar system history simply by choosing appropriate initial temperatures, flow parameters, and orbital initial conditions. For a $\omega_1/\omega_2 \approx 2$ resonance of a given duration (say two byr), for example, we can easily produce runaways that occur at almost any time during the resonance (except the very beginning, before the eccentricity is pumped) simply by varying $T_c(t = 0)$ by a few degrees. Similarly, for a

given temperature at the onset of resonance, we can shift the time of runaway by shifting the time at which the system enters resonance (by altering ω_1 and ω_2 at $t = 0$), on which we have no constraint.

Ganymede's resurfacing took place over perhaps 10^8 years or longer (McKinnon and Parmentier 1986). A possible explanation is that Ganymede passed through *both* the $\omega_1/\omega_2 \approx 1/2$ and $\omega_1/\omega_2 \approx 2$ (or $\omega_1/\omega_2 \approx 1/2$ and 3/2) resonances before evolving into the Laplace resonance (Showman and Malhotra 1997). If thermal runaways occurred during both resonances, two distinct resurfacing episodes could occur, leading to a variation in ages of bright terrain. Another possibility is that thermal heterogeneities in the mantle could allow a sequence of regional runaways, perhaps spread over 10^8 years, which together constitute a single global runaway.

We propose here an alternate scenario that might allow resurfacing in the absence of a runaway. The melting-point viscosities we have used assume a grain size of $d \sim 1$ mm or smaller. In pure ice, however, grains anneal and grow over time, possibly reaching ~1 m over the age of the solar system if the temperature exceeds 200 K (Azuma and Higashi 1983). The assumption of small grain size is based on the uncertain idea that Ganymede's mantle contains enough foreign inclusions (e.g. silicate particles) to limit grain growth. Because $\eta_0 \propto d^2$ (Kirk and Stevenson 1987), absence of such contamination could lead to very high viscosities. η_0 would grow rapidly after satellite formation, soon rising high enough to prevent solid-state convection. Heat loss would be low and Ganymede would enter the resonance in a warm, molten state [by itself, this active state does *not* imply resurfacing; see Showman and Stevenson (1996)]. For $\eta_0 \geq 10^{16}$ Pa sec, viscous dissipation would be minimal, and Q might achieve 100 even though the mantle is very warm. (In contrast, our thermal model predicts $Q \sim 1$ for such a state, for $\eta_0 \sim 10^{13}$ Pa sec.) With $Q \sim 100$, the relevant Laplace-like resonances pump Ganymede's eccentricity to about 0.01 for reasonable Q_J (Showman and Malhotra 1997, Fig. 7). This yields a strain amplitude of 10^{-5} throughout the entire resonance. Thus, resurfacing might occur without a global runaway at all. This scenario has the additional advantage that resurfacing could easily take place over a period of several hundred million years.

If this occurred, Ganymede's ocean should still exist. At the present eccentricity, the variation in height of the tidal bulge over the 1-week orbital period is ~16 m if a large ocean and thin ice I layer exist, but only 1 m if the satellite is fully frozen. This scenario might therefore be tested observationally by measuring the magnitude of changes in the tidal bulge from an orbiting satellite.

Regardless of which thermal model is appropriate (and whether a runaway occurred), time variability of Jupiter's tidal dissipation factor Q_J could make resurfacing far more likely. The only proposed mechanisms for achieving a time-averaged Q_J of 10^5 to 10^6 (necessary for tidal evolution of the resonances) allow Q_J drop to 10^3–10^4 for short periods (Ioannou and Lindzen 1993, Stevenson 1983). If Q_J plummeted to 10^3–10^4 for a short ~10^8-year interval while the system was locked in an eccentricity-pumping resonance, the eccentricity and therefore tidal flexing amplitude would rise. Liquid water could therefore be pumped to the surface from a much greater depth, and regional runaways occurring in lithospheric ice would be far more likely to generate liquid near the surface. The fact that Q_J might exceed 10^6 at other times would not lessen the likelihood of resurfacing during the low-Q_J phase.

Finally, the models proposed here have important implications for the thermal evolution of Ganymede's rock/iron core and hence for producing a magnetic field. The key difficulty lies in explaining how convective motion could occur in a liquid iron core at present (Stevenson 1996, McKinnon 1996). If the Galilean satellites passed through the $\omega_1/\omega_2 \approx 2$ or 3/2 resonance, Ganymede's interior would have become warm and a large internal ocean might have formed regardless of whether a runaway occurred. On disruption of the resonance (followed by capture into the Laplace resonance), dissipative heating would cease and the temperature would plummet at a rate ~30–50 K/Ga for half a billion years or more. Although such cooling is insufficient to drive convection in an iron core with thermal buoyancy (Kuang and Stevenson 1996), convection driven by compositional buoyancy might be possible: the cooling would cause freezing of the solid iron inner core, leaving behind sulfur-rich, buoyant fluid at the base of the liquid iron outer core. Dynamo activity and a magnetic field would ensue. Only after 10^9 years would the thermal "memory" of the tidal heating disappear, at which point convection in the liquid core—and the internally generated magnetic field—would cease. Thus, if significant tidal heating occurred within the past billion years, a modern-day internally generated magnetic field could be explained. This is consistent with the suggestion of E. M. Shoemaker (personal communication, 1995) that Ganymede's grooved terrain, presumably formed during the same heating event, is younger than a billion years. Further, Ganymede's substantial free eccentricity (0.0015) is probably remanent from a previous resonance passage, since neither cometary impacts nor the present Laplace resonance can excite such large values (Showman and Malhotra 1997). As the eccentricity damping time is ~10^8 years for reasonable Q/k, the inferred resonance must have ended less than a billion years ago.

ACKNOWLEDGMENTS

We thank G. Schubert, P. Schenk, and W.B. McKinnon for useful discussions. This research was supported by NASA Grant NAGW-185

and by an NSF graduate fellowship. A portion of this research was done while R.M. was a Staff Scientist and A.P.S. was a Visiting Graduate Fellow at the Lunar and Planetary Institute which is operated by the Universities Space Research Association under Contract NASW-4574 with the National Aeronautics and Space Administration.

REFERENCES

Anderson, J. D., E. L. Lau, W. L. Sjogren, G. Schubert, and W. B. Moore 1996. Gravitational constraints on the internal structure of Ganymede. *Nature* **384,** 541–543.

Azuma, N., and A. Higashi 1983. Effects of hydrostatic pressure on the rate of grain growth in Antarctic polycrystalline ice. *J. Phys. Chem.* **87,** 4060–4064.

Cassen, P., S. J. Peale, and R. T. Reynolds 1980. On the comparative evolution of Ganymede and Callisto. *Icarus* **41,** 232–239.

Dermott, S. F. 1979. Tidal dissipation in the solid cores of the major planets. *Icarus* **37,** 310–321.

Dorsey, N. E. 1940. *Properties of Ordinary Water Substance.* Reinhold, New York.

Durham, W. B., H. C. Heard, and S. H. Kirby 1983. Experimental deformation of polycrystalline H_2O ice at high pressure and low temperature: Preliminary results. *J. Geophys. Res. Suppl.* **88,** B377–B392.

Durham, W. B., S. H. Kirby, and L. A. Stern 1992. Effects of dispersed particulates on the rheology of water ice at planetary conditions. *J. Geophys. Res.* **97,** 20,883–20,897.

Fletcher, N. H. 1970. *The Chemical Physics of Ice.* Cambridge Univ. Press, London.

Friedson, A. J., and D. J. Stevenson 1983. Viscosity of rock–ice mixtures and applications to the evolution of icy satellites. *Icarus* **56,** 1–14.

Greenberg, R. 1987. Galilean satellites: Evolutionary paths in deep resonance. *Icarus* **70,** 334–347.

Hobbs, P. V. 1974. *Ice Physics.* Oxford Univ. Press (Clarendon), London/New York.

Ioannou, P. J., and R. S. Lindzen 1993. Gravitational tides in the outer planets. II. Interior calculations and estimation of the tidal dissipation factor. *Astrophys. J.* **406,** 266–278.

Jones, S. J., and H. A. M. Chew 1983. Creep of ice as a function of hydrostatic pressure. *J. Phys. Chem.* **87,** 4064–4066.

Kirby, S. H., W. B. Durham, M. L. Beeman, H. C. Heard, and M. A. Daley 1987. Inelastic properties of ice Ih at low temperatures and high pressures. *J. Phys. C suppl.* **48,** 227–232.

Kirk, R. L., and D. J. Stevenson 1987. Thermal evolution of a differentiated Ganymede and implications for surface features. *Icarus* **69,** 91–134.

Kivelson, M. G., K. K. Khurana, C. T. Russell, R. J. Walker, J. Warnecke, F. V. Coroniti, C. Polanskey, D. J. Southwood, and G. Schubert 1996. Discovery of Ganymede's magnetic field by the Galileo spacecraft. *Nature* **384,** 537–541.

Kuang, Z., and D. J. Stevenson 1996. Magnetic field generation in the Galilean satellites. *Eos Suppl.* **77,** F437.

Lunine, J. I., and D. J. Stevenson 1982. Formation of the Galilean satellites in a gaseous nebula. *Icarus* **52,** 14–39.

Malhotra, R. 1991. Tidal origin of the Laplace resonance and the resurfacing of Ganymede. *Icarus* **94,** 399–412.

McKinnon, W. B. 1981. Tectonic deformation of Galileo Regio and limits to the planetary expansion of Ganymede. *Proc. Lunar Planet. Sci. Conf. 12th,* 1585–1597.

McKinnon, W. B. 1996. Core evolution in icy satellites. *Eos Suppl.* **77,** F442.

McKinnon, W. B., and E. M. Parmentier 1986. Ganymede and Callisto. In *Satellites* (J. A. Burns and M. S. Matthews, Eds.), pp. 718–763. Univ. of Arizona Press, Tucson.

Munk, W. H., and G. J. F. MacDonald 1960. *The Rotation of the Earth.* Cambridge Univ. Press, London.

Ojakangas, G. W., and D. J. Stevenson 1989. Thermal state of an ice shell on Europa. *Icarus* **81,** 220–241.

Parmentier, E. M., S. W. Squyres, J. W. Head, and M. L. Allison 1982. The tectonics of Ganymede. *Nature* **295,** 290–293.

Peale, S. J. and P. M. Cassen 1978. Contribution of tidal dissipation to lunar thermal history. *Icarus* **36,** 245–269.

Peale, S. J., P. Cassen, and R. T. Reynolds 1979. Melting of Io by tidal dissipation. *Science* **203,** 892–894.

Reynolds, R. T., and P. M. Cassen 1979. On the internal structure of the major satellites of the outer planets. *Geophys. Res. Lett.* **6,** 121–124.

Ross, M. N. and G. Schubert 1987. Tidal heating in an internal model of Europa. *Nature* **325,** 133–134.

Schubert, G., D. J. Stevenson, and K. Ellsworth 1981. Internal structures of the Galilean satellites. *Icarus* **47,** 46–59.

Shoemaker, E. M., and R. F. Wolfe 1982. Cratering time scales for the Galilean satellites. In *Satellites of Jupiter* (D. Morrison, Ed.), pp. 277–339. Univ. of Arizona Press, Tucson.

Showman, A. P., and R. Malhotra 1997. Tidal evolution into the Laplace resonance and the resurfacing of Ganymede. *Icarus* **127,** 93–111.

Showman, A. P., and D. J. Stevenson 1996. Resurfacing of Ganymede and other icy satellites by passage through orbital resonance. *Icarus*.

Solomatov, V. S. 1995. Scaling of temperature- and stress-dependent viscosity convection. *Phys. Fluids* **7,** 266–274.

Squyres, S. W. 1980. Volume changes in Ganymede and Callisto and the origin of grooved terrain. *Geophys. Res. Lett.* **7,** 593–596.

Squyres, S. W. 1982. The evolution of the tectonic features on Ganymede. *Icarus* **52,** 545–559.

Stevenson, D. J. 1983. Anomalous bulk viscosity of two-phase fluids and implications for planetary interiors. *J. Geophys. Res.* **88,** 2445–2455.

Stevenson, D. J. 1996. When Galileo met Ganymede. *Nature* **384,** 511–512.

Tittemore, W. C. 1990. Chaotic motion of Europa and Ganymede and the Ganymede–Callisto dichotomy. *Science* **250,** 263–267.

Weast, R. C. (Ed.) 1987. *CRC Handbook of Chemistry and Physics*, 68th ed. Chemical Rubber Co., Boca Raton, FL.

Weertman, J. 1973. Creep of ice. In *Physics and Chemistry of Ice* (E. Whalley, S. J. Jones, and L. W. Gold, Eds.), pp. 320–337. Roy. Soc. of Canada, Ottowa.